

# Off-diagonal correlations in a one-dimensional gas of dipolar bosons

Tommaso Roscilde<sup>1</sup> and Massimo Boninsegni<sup>2</sup>

<sup>1</sup> Laboratoire de Physique, Ecole Normale Supérieure de Lyon, 46 Allée d'Italie, 69007 Lyon, France

<sup>2</sup> Department of Physics and Astronomy, University of Alberta, 248L CEB, 11322-89 Ave, Edmonton, Alberta T6G 2G7, Canada

PACS numbers: 03.75.Ss, 71.10.Pm, 74.20.Mn, 42.50.-p

**Abstract.** We present a quantum Monte Carlo study of the one-body density matrix (OBDM) and the momentum distribution of one-dimensional dipolar bosons, with dipole moments polarized perpendicular to the direction of confinement. We observe that the long-range nature of the dipole interaction has dramatic effects on the off-diagonal correlations: although the dipoles never crystallize, the system goes from a quasi-condensate regime at low interactions to a regime in which quasi-condensation is discarded, in favor of quasi-solidity. For all strengths of the dipolar interaction, the OBDM shows an oscillatory behavior coexisting with an overall algebraic decay; and the momentum distribution shows sharp kinks at the wavevectors of the oscillations,  $Q = \pm 2\pi n$  (where  $n$  is the atom density), beyond which it is strongly suppressed. This *momentum filtering* effect introduces a characteristic scale in the momentum distribution, which can be arbitrarily squeezed by lowering the atom density. This shows that one-dimensional dipolar Bose gases, realized e.g. by trapped dipolar molecules, show strong signatures of the dipolar interaction in time-of-flight measurements.

## 1. Introduction

Trapped quantum degenerate gases are currently offering the possibility of a thorough investigation of fundamental models of correlated quantum liquids, spanning a wide range of regimes from weak to strong interactions [1]. A particularly appealing aspect of cold atoms is indeed the tunability of the interparticle interactions. So far most of the experiments have been performed in a regime in which the interaction can be faithfully described as a contact  $s$ -wave interaction; tuning an applied magnetic field close to a Feshbach resonance allows to control continuously the magnitude and sign of the associated  $s$ -wave scattering length [2]. The use of Feshbach resonances allows in particular to suppress almost completely the contact interaction, leading to the observation of the effects of weaker magnetic dipole-dipole interactions for atoms which have a net magnetic moment, such as  $^{52}\text{Cr}$  [3, 4, 5]. On the other hand, the recent realization of a stable degenerate gas of heteronuclear molecules [6] appears to

pave the way to the exploration of the physics of quantum fluids with strong (and variable) electric dipole-dipole interactions; in fact the application of an electric field on the heteronuclear molecules, or the dressing of molecules with a microwave field, can induce a tunable electric dipole.

On the theoretical side, the presence of the dipolar interaction has been shown to lead to many intriguing effects when the system is confined to two spatial dimensions, such as roton-like excitations in the liquid regime [7], spontaneous crystallization [8], and even supersolidity in presence of an optical lattice [7]. In the case of dipolar bosons confined to one spatial dimension, in the absence of an optical lattice Mermin-Wagner-Hohenberg theorem forbids crystallization even at  $T = 0$  due to unboundedly strong quantum fluctuations. Hence the system can be described as a Luttinger liquid for all strengths of the dipolar interaction [9, 10, 11, 12]. While it can develop arbitrarily strong diagonal correlations, resulting in a so-called super-Tonks behavior [13, 14], such correlations are always decaying as a power of the distance.

All the existing studies of the one-dimensional dipolar Bose gas have mainly focused on diagonal correlations and on the static structure factor [9, 10, 12, 13, 14]. Yet the most natural observables in cold atom experiments are off-diagonal correlations, namely the one-body density matrix (OBDM) and its Fourier transform, the momentum distribution, which is obtained from time-of-flight measurements. In this paper we focus our attention on these quantities, which we compute numerically exactly by quantum Monte Carlo simulations. In particular, we show that off-diagonal correlations exhibit very strong signatures of dipolar physics. In fact the OBDM has a characteristic oscillatory behavior at the ordering vector  $Q$  of the Wigner crystal obtained in the classical limit. Such a behavior translates into a strong feature in the momentum distribution, namely a sharp kink at the  $Q$  vector, and a strong suppression of the momentum population for larger wavevectors. This effect of momentum filtering in the range  $[-Q, Q]$  is completely controlled by the density of the system, so that the momentum distribution can be arbitrarily squeezed in momentum space, although the system *never* attains condensation at finite density. A study of the two-body problem suggests that momentum filtering is a special feature of long-range interactions already at the few-body level, although its manifestation in the  $N$ -body problem is much more pronounced.

The paper is structured as follows. Section 2 describes the system Hamiltonian and the numerical method; Section 3 presents a study of off-diagonal correlations in the two-body problem with dipolar interactions, contrasting it with the case of contact interactions; Section 4 focuses on the OBDM as compared to predictions from Luttinger liquid theory; and finally Section 5 discusses the results concerning the momentum distribution.

## 2. Model and methods

We investigate a system of  $N$  bosons confined to a one dimensional box of length  $L$  with periodic boundary conditions. The system Hamiltonian reads

$$\mathcal{H} = -\frac{\hbar^2}{2m} \sum_{i=1}^N \frac{d^2}{dx_i^2} + \sum_{i<j} V(x_i - x_j) . \quad (1)$$

In the following, otherwise specified, we will focus on the dipolar potential

$$V_{\text{dip}}(x - x') = \frac{V_d}{|x - x'|^3} \quad (2)$$

Introducing the particle density  $n = N/L$  and the rescaled variables  $\tilde{x}_i = x_i/r_0$  (where  $r_0 = mV_d/\hbar^2$  is an effective length associated with the potential), the Hamiltonian with dipolar interactions can be rewritten in the convenient form

$$\mathcal{H}(\text{Ryd}) = (nr_0)^2 \left[ -\frac{1}{2} \sum_{i=1}^N \frac{d^2}{d\tilde{x}_i^2} + (nr_0) \sum_{i<j} \frac{1}{|\tilde{x}_i - \tilde{x}_j|^3} \right] . \quad (3)$$

Here the Hamiltonian is expressed in effective Rydberg units,  $\text{Ryd} = \hbar^2/(mr_0^2)$  [15]. Hence  $nr_0$  gives the dimensionless strength of the dipolar potential, and it contains a fundamental property of scale invariance, typical of power-law decaying potentials: rescaling the density  $n \rightarrow n/\lambda$  and the effective length  $r_0 \rightarrow \lambda r_0$ , the physics of the system is unchanged (apart from a rescaling of the box length,  $L \rightarrow \lambda L$ , and, accordingly, of the positions,  $x \rightarrow \lambda x$ ). In the following we will compare the behavior of the dipolar system with that of the Lieb-Liniger gas, characterized by the  $\delta$ -potential

$$V_\delta(x - x') = g \delta(x - x') . \quad (4)$$

with repulsive nature,  $g > 0$ . The associated scattering length is given by  $a = -2\hbar^2/(mg)$ . The dimensionless strength of the potential can be measured by  $(n|a|)^{-1}$ .

We investigate the ground-state properties of the 1D gas of dipolar bosons by quantum Monte Carlo simulations, based on the continuous-space Worm Algorithm, which allows one to obtain the one-body density matrix straightforwardly [16, 17]. While the method is strictly valid for finite temperatures only, the zero temperature behavior can be recovered for low enough temperatures. In addition to Monte Carlo simulations, we also use standard exact diagonalization to study the problem of two interacting bosons, whose results are presented in the next section.

## 3. Two-body problem

The study of the off-diagonal correlations of the two body problem turns out to be quite insightful in the perspective of the  $N$ -body problem, as some fundamental traits of the latter are already exhibited by the former. We numerically evaluate the ground-state wavefunction  $\phi(r)$  for the relative coordinate of the two-body problem on a  $L = 2l$  ring (where  $l$  is an arbitrary length unit), and the associated momentum distribution

$$n(k) = \frac{2}{L} \left| \int dr e^{ikr} \phi(r) \right|^2 \quad (5)$$

defined on discrete momenta  $k = 2\pi p/L$ ,  $p \in Z$ .

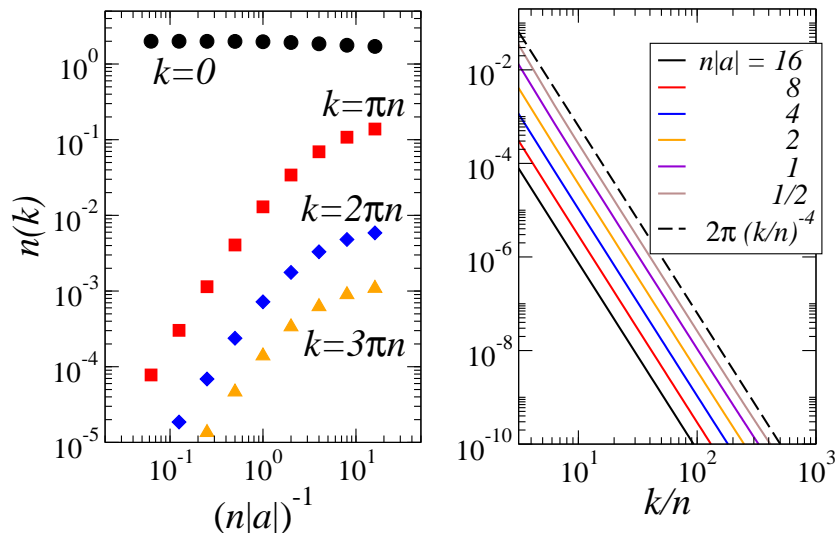


**Figure 1.** *Left panel:* Occupation of the lowest momentum states as a function of the interaction strength for the ground state of two bosons interacting via a  $\delta$ -potential. We observe that the weight lost at  $k = 0$  is distributed over all momenta. *Right panel:* Momentum distribution for varying strength of the  $\delta$  potential.

We begin our analysis of the two-body problem by investigating the Lieb-Liniger two-body problem, whose results are shown in Fig. 1. The evolution of the momentum distribution with increasing strength of the potential term (decreasing  $n|a|$ ) shows a depletion of the  $k = 0$  contribution, and an increase of all the finite-momentum components, compatible with a gradual squeezing of the two-body wavefunction  $\phi(r)$  in real space. In particular for all strengths of the interaction, the momentum distribution shows a characteristic decay as  $1/k^4$  for all finite momenta – a behavior which is consistent with that of the large- $k$  tail of  $n(k)$  in the  $N$ -body problem [18]. This means that an increasing interaction strength is simply imposing a global rescaling factor to the momentum distribution at finite  $k$ .

The behavior in the dipolar case is radically different, as shown in Fig 2. First of all, in the limit  $nr_0 \rightarrow 0$  the system maintains a finite occupation of non-zero momentum states, due to the fact that, in this limit, dipolar bosons reproduce the physics of the Tonks-Girardeau gas of impenetrable particles [10, 14] (see Sec. 5 for further discussion). Moreover, upon increasing the potential strength  $nr_0$  we observe not only a suppression of the  $k = 0$  momentum component, but also at *finite* momenta  $|k| \geq Q = 2\pi n$ , at least for moderate potential strength. Hence the increase of finite momentum components, associated with the squeezing of the two-body wavefunction in real space, is highly

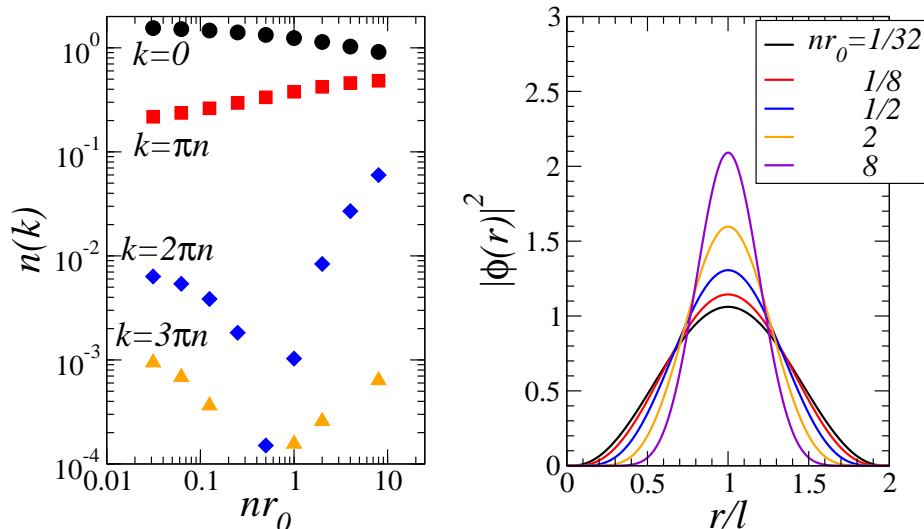


**Figure 2.** *Left panel:* Occupation of the lowest momentum states for the ground state of two bosons interacting via a dipolar potential. We observe that, for increasing interactions, the population lost at momentum  $k = 0$  is mainly transferred to momentum  $k = \pi n$ , while the population at higher momenta can be even suppressed. This behavior is to be contrasted with that of contact interactions, Fig. 1. *Right panel:* Square modulus of the two-body wavefunction.

inhomogeneous, and it only takes place within a momentum window  $0 < k < Q$ , while the momentum components out of this window are strongly suppressed. This inhomogeneous redistribution of populations in momentum space, driven by increasing the interaction, results in a peculiar momentum filtering effect, which is present in an even more dramatic fashion in the  $N$ -body problem, as it will be discussed in Sec. 5.

#### 4. One-body density matrix

The one-body density matrix (OBDM)

$$C(x - x') = \langle \psi^\dagger(x) \psi(x') \rangle \quad (6)$$

for a system of  $N$  dipolar bosons in a box of length  $L = Nl$  with periodic boundary conditions, has been investigated via quantum Monte Carlo simulations, for interaction strengths ranging between  $nr_0 = 0.2$  and  $nr_0 = 5$ . The number of particles utilized for the results shown here is  $N=30$ , but we performed calculations with  $N=15$  and  $N=60$  as well, in order to gauge the importance of finite-size effects. We generally find that simulations at a temperature  $k_B T \lesssim 0.1 nr_0$  Ryd do not show any significant thermal effect, and all results presented in the paper are referred to this temperature range.

Fig. 3 shows the OBDM for two representative values of the potential strength  $nr_0$ . Strong quantum fluctuations in one dimension strongly suppress correlations, so that the OBDM displays an algebraic decay. In addition to this behavior, we observe an oscillation with period  $1/n$ , revealing the strong role played by interactions. Indeed, as we will see later, interactions lead to arbitrarily strong diagonal correlations, which imply a crystalline structure of the particles at short range. This structure is reflected in the OBDM, which exhibits a modulation with an amplitude that decays spatially in the same way as the density correlations.

According to the general Luttinger liquid theory, density-density correlations in a boson liquid display a dominant decaying behavior at large distances in the form [19]:

$$G(x - x') = \langle \rho(x)\rho(x') \rangle \sim \frac{\cos[Q(x - x')]}{d(x - x'|L)^{2K}} \quad (7)$$

where  $K$  is the Luttinger liquid exponent;  $Q = 2\pi n$  is the ordering vector of the classical Wigner crystal; and  $d(x|L) = L|\sin(\pi x/L)|/\pi$  is the cord function. On the other hand, the OBDM is predicted to exhibit the following (asymptotic) decay [19]:

$$C(r) \xrightarrow{r \rightarrow \infty} \frac{1}{d(r|L)^{1/(2K)}} \left[ b_0 + b_1 \frac{\cos(Qr)}{d(r|L)^{2K}} + \sum_{m=2}^{\infty} b_m \frac{\cos(mQr)}{d(r|L)^{2m^2K}} \right]. \quad (8)$$

Hence, besides the dominant decay of the type  $|r|^{-1/(2K)}$ , the OBDM may also show a modulation at wavevector  $Q$  with an amplitude decaying as the density-density correlations,  $|r|^{-2K}$ , and modulations at higher harmonics  $mQ$  with increasingly faster decay. We can successfully fit our numerical results to Eq. 8, and we are able to resolve harmonics up to  $m = 2$  within our numerical precision. In particular, for the coefficient  $b_1$  of the lowest harmonic we obtain *negative* values ranging in the interval  $b_1 \sim -3 \div 5 \times 10^{-2}$ . The negativity of this coefficient has important consequences for the shape of the momentum distribution, as will be discussed in the next section.

In addition, fits to Eq. 8 allow to extract the exponent  $K$ , which is plotted in Fig. 4 as a function of the interaction strength  $nr_0$ .  $K$  has the fundamental property of governing the scaling of the peak in the momentum distribution and in the static structure factor with increasing system size. Introducing the momentum distribution

$$n(k) = \frac{1}{L} \int_0^L dr C(r) e^{ikr} \quad (9)$$

and the static structure factor

$$S(k) = \frac{1}{L} \int_0^L dr G(r) e^{ikr} \quad (10)$$

one obtains that  $n(k = 0) \sim L^{1-1/(2K)}$ , while  $S(k = Q) \sim L^{1-2K}$ . According to the general definitions, the system exhibits *quasi-condensation* when the peak in the momentum distribution diverges with system size ( $K > 1/2$ ); and it exhibits *quasi-solidity* when the peak in the structure factor diverges ( $K < 1/2$ ). As shown in Fig. 4, increasing dipolar interactions allow to continuously vary the  $K$  exponent from  $K = 1$  in the weakly interacting regime (characterized by fermionization [10, 14]), to

$K \rightarrow 0$  in the strongly interacting regime. In particular we find that for  $nr_0 \approx 1.3$  the Luttinger exponent crosses the value  $K = 1/2$ , corresponding to a transition from quasi-condensation to quasi-solidity. Hence dipolar interactions allow to continuously tune the role of correlations, driving the system from a regime of dominant off-diagonal correlations to a regime of dominant diagonal ones. Our estimate of the  $K$  exponent stemming from the OBDM is in good agreement with the semi-analytic formula given in Ref. [10], extracted from a fit to quantum Monte Carlo results for the ground state energy.

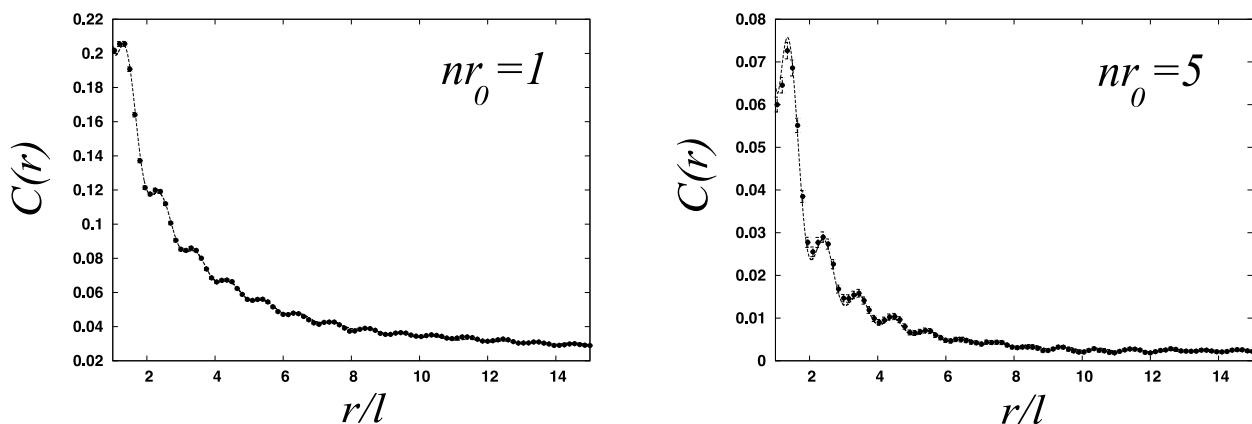


**Figure 3.** One-body density matrix for  $N = 30$  dipolar bosons. The dashed lines are fits to the Luttinger liquid formula, Eq. (8), truncated to the  $m = 2$  order.

## 5. Momentum distribution

The evolution of the momentum distribution, Eq. 9, upon changing the interaction strength  $nr_0$  is shown in Figs. 5 and 6. As discussed in the previous section, the OBDM exhibits a modulation term at wavevector  $Q$  with a *negative* prefactor. This means that the corresponding feature in the momentum distribution is to be expected as a dip at the same wavevector. Indeed, the momentum distribution shows a sharp kink at  $k = Q$ , but it also shows a strong suppression of the momentum population at all momenta  $|k| > Q$ , observed for all investigated values of  $nr_0$ . Hence we observe that the dipolar interaction introduces a characteristic scale  $Q$  in the momentum distribution, and a momentum filtering effect outside of the interval  $[-Q, Q]$ . This is to be contrasted with the case of contact interactions: indeed the Lieb-Liniger model has a momentum distribution with power-law wings,  $n(k) \sim k^{-4}$  [18], and hence it does not contain any special momentum scale. The momentum filtering effect has the characteristic feature that, upon increasing the interaction strength  $nr_0$ , the weight lost in the  $k = 0$  peak is redistributed almost exclusively over the  $[-Q, Q]$  interval, similarly to what we have observed in the case of

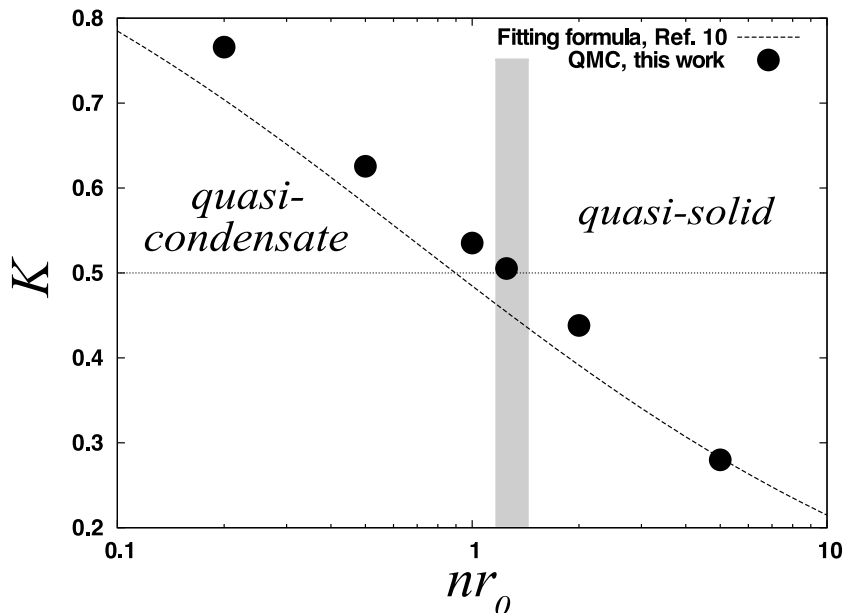


**Figure 4.** Luttinger liquid exponent  $K$  as a function of the interaction strength  $nr_0$ . The shaded region marks the transition from quasi-condensation to quasi-solidity.

the two-body problem. As a result, the strongly peaked distribution at low  $nr_0$  evolves into an almost triangular distribution for stronger  $nr_0$ . For extremely large values of  $nr_0$  one might expect that the weight lost at  $k = 0$  will eventually start redistributing over a broader interval than  $[-Q, Q]$ . Nonetheless the persistence of Luttinger liquid behavior in the system for arbitrary large values of  $nr_0$  leads us to conclude that the characteristic periodic modulation of the OBDM, responsible for the suppression of the momentum distribution around  $q = Q$ , will also persist to much larger values of  $nr_0$  than the ones considered here, so that the momentum distribution will maintain a strong signature of dipolar physics around that momentum value.

Momentum filtering can be probed experimentally in two different setups. Working at constant density  $n$ ,  $nr_0$  can be controlled by increasingly polarizing the dipoles and hence increasing  $r_0$ . This leads to the observations of Fig. 5, in which the momentum distribution is always defined on the same support and it changes shape from strongly peaked to triangular. A second type of experiment can be carried out at fixed dipole polarization, by changing the dipole density  $n$ , *e.g.* by varying the trapping potential which holds the system. Fig. 6 illustrates such a protocol, which allows to shrink arbitrarily the support  $[-Q, Q]$  of the momentum distribution by lowering the trapping frequency, and hence to concentrate all the atoms to an arbitrarily small volume in momentum space. Yet paradoxically the system never condenses; quite oppositely, as discussed in Refs. [10] and [14], it *fermionizes* in the limit  $nr_0 \rightarrow 0$ , reproducing the behavior of a Tonks-Girardeau gas.



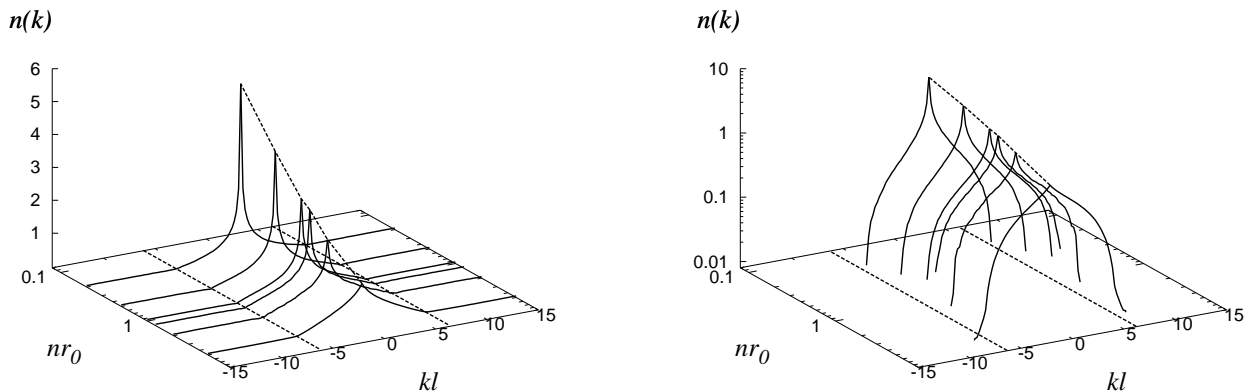


**Figure 5.** Momentum distribution as a function of the interaction strength  $nr_0$  for a system with *fixed density*  $n = 1/l$ . The dashed lines mark the momenta  $Q = \pm 2\pi n$ . The right panel shows the distribution in logarithmic scale, to evidence the sharp suppression for momenta  $|k| > Q$ .

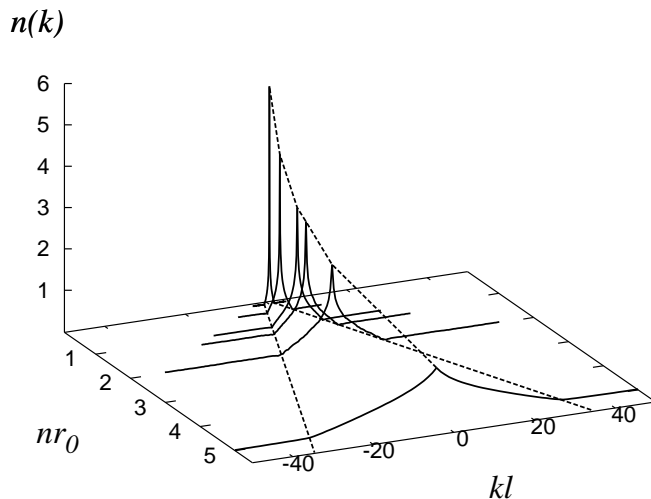


**Figure 6.** Momentum distribution as a function of the interaction strength  $nr_0$  for a system with *fixed dipoles*, namely a constant  $r_0$ . Here the number of particles is fixed to  $N = 30$ , and the system size changes when changing  $nr_0$ , and it goes from  $L = 150l$  for  $nr_0 = 0.2$  to  $L = 6l$  for  $nr_0 = 5$ .

## 6. Experimental realization

The momentum distribution is notoriously the most accessible quantity in trapped gas experiments, simply obtained by time-of-flight measurements [1]. More challenging is the realization of a quantum degenerate gas with dominantly dipolar interactions [7].

Quantum degeneracy has been achieved in  $^{52}\text{Cr}$  [3, 4, 5], for which  $s$ -wave interactions can be suppressed by a Feshbach resonance in favor of residual magnetic dipolar interactions. In this system one has  $V_d = \mu_0 \mu_m^2 / (4\pi)$  where  $\mu_m = 6\mu_B$  (Bohr magneton) is the magnetic moment of  $^{52}\text{Cr}$ , and consequently  $r_0 = 2.7 \times 10^{-9}$  m. For characteristic condensate densities of  $10^{13} \text{ cm}^{-3}$  we obtain linear densities  $n \approx 2 \times 10^6 \text{ m}^{-1}$ , and an effective potential strength  $nr_0 \approx 0.5 \times 10^{-2}$ , which does not allow to explore the transition from quasi-condensation to quasi-solidity described in this paper, but it might be already sufficient to observe effects of momentum filtering. Polar molecules, on the other hand, can potentially feature dipolar interactions with characteristic lengths  $r_0$  which are 3 orders of magnitude higher than those for  $^{52}\text{Cr}$  [7], and they would hence allow to fully span the regime of interactions described in this paper.

Another potentially challenging issue is the confinement of dipolar gases in one dimensional traps. Indeed confining the gas in an array of tubes created by a two-dimensional optical lattice leads to *quasi*-one-dimensional systems, with sizable residual inter-tube coupling due to the long-range nature of dipolar interactions. A possible solution is the use of largely spaced tubes, obtained via two-dimensional optical lattices created by crossing lasers at an angle far smaller than  $\pi$ . Another solution is trapping in single-mode tight atom waveguides created *e.g.* by atom chips [20].

## 7. Conclusions

In this paper we have investigated the effect of dipolar interactions on the off-diagonal correlations of a one-dimensional Bose gas. We have shown that the long-range nature of dipolar interactions changes radically the momentum distribution with respect to the case of contact interactions, introducing a characteristic momentum scale beyond which the momentum distribution is strongly suppressed. The effect of momentum filtering is fully controlled by the gas density, and it allows to squeeze the momentum distribution to an arbitrarily small portion of momentum space. The momentum distribution can also reveal the interaction-induced transition from quasi-condensation to quasi-solidity, via the loss of scaling of the zero-momentum peak with system size. All the phenomena discussed in this paper can be observed via time-of-flight measurements on polar molecules trapped in largely spaced two-dimensional optical lattices, or in tight atom waveguides.

## 8. Acknowledgements

We acknowledge very fruitful discussions with E. Orignac, and we are indebted to M. Dalmonte for pointing out a mistake in the comparison of our data with those of Ref. [10]. This work was supported in part by the Natural Science and Engineering Research Council of Canada under research grant 121210893, and by the Alberta Informatics Circle of Research Excellence (iCore). MB gratefully acknowledges the support of CNRS and the hospitality of the Ecole Normale Supérieure de Lyon during a long-term visit,

in which part of this work was completed.

- [1] Bloch I, Dalibard J, and Zwirger W 2008, *Rev. Mod. Phys.* **80**, 885.
- [2] Chin C, Grimm R, Julienne P, and Tiesinga E 2009, arXiv:0812.1496.
- [3] Lahaye T, Koch T, Fröhlich B, Fattori M, Metz J, Griesmaier A, Giovanazzi S, and Pfau T 2007, *Nature* **448**, 672.
- [4] Koch T, Lahaye T, Metz J, Fröhlich B, Griesmaier A, and Pfau T, *Nat. Phys.* **4**, 218 (2008).
- [5] Lahaye T, Metz J, Fröhlich B, Koch T, Meister M, Griesmaier A, Pfau T, Saito H, Kawaguchi Y, and Ueda M 2008, *Phys. Rev. Lett.* **101**, 080401.
- [6] Ni K K, Ospelkaus S, de Miranda M H G, Pe'er A, Neyenhuis B, Zirbel J J , Kotochigova S, Julienne P S, Jin D S, and Ye J 2008 *Science* **322**, 231.
- [7] For a recent review, see Lahaye T, Menotti C, Santos L, Lewenstein M, and Pfau T 2009, arXiv:0905.0386.
- [8] Büchler H P, Demler E, Lukin M, Micheli A, Prokof'ev N, Pupillo G, and Zoller P 2007, *Phys. Rev. Lett.* **98**, 060404.
- [9] Citro R, Orignac E, De Palo S, and Chiofalo M L 2007, *Phys. Rev. A* **75**, 051602.
- [10] Citro R, De Palo S, Orignac E, Pedri P, and Chiofalo M L 2008, *New J. Phys.* **10**, 045011.
- [11] Pedri P, De Palo S, Orignac E, Citro R, and Chiofalo M L 2008, *Phys. Rev. A* **77**, 015601.
- [12] De Palo S, Orignac E, Citro R, and Chiofalo M L 2008, *Phys. Rev. B* **77**, 212101.
- [13] Arkhipov A S, Astrakharchik G E, Belikov A V, and Lozovik Y E 2005, *JETP Lett.* **82**, 39.
- [14] Astrakharchik G E and Lozovik Y E 2008, *Phys. Rev. A* **77**, 013404.
- [15] Our definitions of  $r_0$  and Ryd are slightly different from those of, *e.g.*, Refs. [9, 10, 11, 12]. There  $r_0 = 2mV_d^2/\hbar^2$  and Ryd =  $\hbar^2/(2mr_0^2)$ . Consequently the Hamiltonian, Eq. (3), differs by a factor of 1/2 in the kinetic term.
- [16] Boninsegni M, Prokof'ev N V, and Svistunov B V 2006, *Phys. Rev. Lett.* **96**, 070601.
- [17] Boninsegni M, Prokof'ev N V, and Svistunov B V 2006, *Phys. Rev. E* **74**, 036701.
- [18] Olshanii M and Dunjko V 2003, *Phys. Rev. Lett.* **91**, 090401.
- [19] Cazalilla M 2004, *J. Phys B* **37**, S1-S47.
- [20] Thywissen J H, Olshanii M, Zabow G, Drndić M, Johnson K S, Westervelt R M, and Prentiss M 1999, *Eur. Phys. J. D* **7**, 361.